



SMR/917 - 14

**SECOND WORKSHOP ON
SCIENCE AND TECHNOLOGY OF THIN FILMS**

(11 - 29 March 1996)

"Sample preparation aspects for TEM characterization of grain boundaries and interfaces."

presented by:

G. RADNÓCZI

Research Institute for Technical Physics

Hungarian Academy of Sciences

P.O. Box 76

Foti Ut. 56

H-1325 Budapest

Hungary

These are preliminary lecture notes, intended only for distribution to participants.

Sample Preparation Aspects for TEM Characterization of Grain Boundaries and Interfaces¹

György Radnóczy

Research Institute for Technical Physics of the
Hungarian Academy of Sciences

H-1325 Budapest, P. O. Box 76, Hungary

radnoczi@mufi.hu

ABSTRACT

The theory of surface morphology development during low angle ion milling for transmission electron microscopy is discussed from the point of view of preparing samples containing grain boundaries and heterophase interfaces. The basic steps of the mechanical preparation and the consequences of the ion beam-sample movement geometry are also listed. An example of 10 μm diamond/Si is shown to illustrate the power of the technique.

INTRODUCTION

The most widely used sample preparation technique for inhomogeneous materials is ion milling. The basic reason for this is, that the systems- the films and substrate- are usually composed of materials different in chemical nature and so not an ideal subject to chemical or electrochemical methods. Low angle ion milling combined with a dedicated embedding procedure and sample rotation or/and rocking during ion milling can provide the desired samples from almost all kinds of layer interfaces and layer structures [1,2].

Another applicable technique is the cleavage technique usable for materials on cleaving substrates. These substrates are the A^{III}B^V semiconductor and Si single crystals. The not very ductile films cleave together with their substrate and are good for XTEM investigation in the as-cleaved state. The advantage of the cleaved samples is, that no ion damage of the sample, often occurring in the case of ion milling, is to be expected. The disadvantage of the cleaved samples is, that the thin area is rather

¹ Prepared on the basis of the material of Ref [2]

small, and there is a strong, though known thickness gradient in the sample [3]. However, chemical or electrochemical thinning can also be used in the case of materials, when a chemically compatible solvent for all components of the structure can be found. This is the case for A^{III}B^V quantum well structures e.g. [4].

In general the today techniques of the cross section preparation provide sufficiently good samples which display a thin and large enough area of the whole thickness of the investigated layer structure together with the substrate for TEM study so that artificial preparation effects can mostly be avoided.

Here we shall discuss in detail only the ion milling technique and its use for inhomogeneous materials, i.e. materials containing homo- and heterophase interfaces.

THEORY

The most essential requirement of TEM is that samples were smooth even at the interfaces and free from artifacts. One of the most powerful techniques of preparing such samples for TEM and X-TEM is low angle ion beam thinning. Especially, to get specimens with uniformly thick, transparent regions we have to apply glancing angle ion beams during thinning. The theoretical foundation of this technique has been worked out by Á. Barna [1] by constructing a geometrical model describing the changes of the surface topography during ion beam sputtering. This theory revealed that in the case of low incidence angles the changes of the surface topography lead to the polishing of the surface due to the lateral movement and annihilation of surface steps.

A useful technique of mechanical sample preparation before ion milling as well as a flexible ion milling geometry have also been developed, which make possible the utilization of the advantages, offered by the theory also for cross-sectional preparation.

The model developed and used in [1] describes the specimen surface as steps and smooth plateaus, in a manner similar to those described in Refs. [5,6].

When such a model is being constructed a number of simplifications must be made:

- 1) The surface roughening by ion beams is a macroscopic process, thus a geometrical treatment is sufficient. Singularities of the topography, such as atomically sharp edges and peaks do not develop by ion beam etching, partly because of re-deposition of sputtered atoms [7], partly because of enhanced surface diffusion [8] as well as because of the transmission sputtering effect [9].

- 2) There is no need to develop a three-dimensional treatment, although it would be possible [10], because the measured and calculated dependence of ion beam sputtering speed of materials on the angle of beam incidence scatter nearly one order of magnitude [11].
- 3) The ion milled material is supposed to be homogeneous. This is true for all single crystalline samples as well as for large single crystalline grains in polycrystalline ones. (The effect of inhomogeneities in the sputtering rate, occurring at the interfaces due to orientation and composition effect will be treated additionally.) The ion beam channeling effect is also neglected because of homogenizing effect of surface amorphisation.
- 4) The model does not consider the effect of ion beam shadowing of the steps because, in the most cases, it is only a transient effect at the beginning of the thinning.

The basic surface geometrical elements of the model are inclined macro facets, separating the smooth surface plateaus creating a surface with steps (fig. 1.). These steps are characterized in the model by the angle of their facet $\pm\alpha$ and by their height. The flat plateaus called as valleys and hills of the surface are separated by these inclined steps. The surface has a certain roughness which is taken into account by the angle and height of the facets and lateral size of the hills and valleys.

To calculate the changes of the surface topography the following input parameters of the model should be considered: the sample movement (stationary, rocked or rotated), the arrangement of ion sources (fig. 2.) and the normalized sputtering speed $V(\theta)/V(0)$ as a function of ion beam incidence angle θ (fig. 3.).

When a homogeneous material is sputtered while it is rotated around its surface normal, the flat areas are sputtered uniformly, and their sputtering speed $V(\theta)$ depends on the ion energy and on the ion beam incidence angle θ . θ is measured from the average surface normal. The inclined facets are also sputtered with a speed $V(\alpha,\theta,\omega)$ depending for a given ion energy, on the inclination angle (α), sample position (ω) and on the ion beam incidence angle (fig. 2.). To calculate $V(\alpha,\theta,\omega)$ the equations of Ref. [6] are applicable. Using the above notations:

$$V(\alpha, \theta, \omega) = \frac{1}{2\omega} \int_{-\omega}^{+\omega} V(\arccos(\cos \theta * \cos \alpha + \sin \theta * \sin \alpha * \cos \omega)) d\omega \quad (1)$$

where ω is the angle of rotation of the sample relative to the ion beam.

Eq. 1. is valid for both rotation and oscillation movement. For rotation $\omega = \pm\pi$, for oscillation $|\omega| < \pm\pi$.

The sputtering speed of the inclined facets has a vertical and a lateral component relative to the sample surface. This means that the steps are sputtered down together with the flat areas and are also moving in lateral direction. The speed of this lateral movement for a given ω value can be described with the help of $V(\alpha, \theta, \omega)$ and $V(\theta)$.

$$S_m(\alpha, \theta) = \frac{[V(\alpha, \theta, \omega) / \cos \alpha] - V(\theta)}{\operatorname{tg} \alpha} \quad (2)$$

The sign of this function describes the type of surface development. If S_m is positive the hills are annihilated and the walleyes are broadened. If S_m is negative the walleyes are annihilated and the hills are broadened (fig. 1.). Considering these processes on large surface areas and for rotating sample the overall result of them is that the plateaus are broadening and the number of steps is decreasing, i.e. polishing of the surface occurs. The quantity, which describes the efficiency of this process, $SR(\alpha, \theta)$, is the ratio of the lateral movement speed of the inclined steps $S_m(\alpha, \theta)$, calculated for the actual sample movement, to the vertical sputtering speed of the material $V(\theta)$.

$$SR(\alpha, \theta) = S_m(\alpha, \theta) / V(\theta) \quad (3)$$

Since $V(\theta)$ is always positive the sign of this function is determined by the sign of S_m .

The ideal behavior of $SR(\alpha, \theta)$ can be deduced from its definition. The sample movement must be carried out in such a way, as to achieve the best polishing conditions, i.e. $SR(\alpha, \theta)$ must be large for all values of α and θ . The shape of an ideal $SR(\alpha, \theta)$ dependence for a rotating and rocking sample is shown in fig. 4.

Taking the experimental values of $V(\theta)$ from fig. 3, one can calculate the appropriate $SR(\alpha, \theta)$ dependencies for Si for different sample movement and gun arrangement conditions. Typical results calculated for Si, rotating as well as rocking around the ion beam direction are shown in fig. 5. The optimal ion beam incidence angles for polishing conditions can be considered those, for which $SR(\alpha, \theta)$ has the highest values for most broad interval of α . As we can see from fig. 5a and 5b., the highest values of θ , i.e. the grazing incidences of the ion beam provide the best approach to the ideal curve, shown in fig. 4. Above 85° the absolute value of SR increases rapidly in the whole range of α . This is

the region where reasonable polishing can be realized. The second important observation is that for θ between 0° and 83° the absolute value of SR is more or less equal or less than 1 in the whole range of α , which means that almost no or very little polishing takes place (fig. 5a.). Special θ angles are 45° and 75° where SR is about zero in the whole range of α and this means that the original surface topography is conserved during sputtering, so a rough surface remains rough, and a smooth stays smooth. The utilization of this latter case is not straightforward, because sample inhomogeneities (differences in $V(\theta)$) occur for most TEM samples.

Also there is a dependence on sample movement. The $SR(\alpha, \theta)$ curves reach their highest value for stationary sample, lower for rocking, and lowest for the rotation of the sample (fig. 5c.). However, in the case of rotation, steps of all directions are moving so polishing for steps in all directions takes place, while for a stationary sample steps, parallel to the ion beam do not move, that is remain on their place. Rocking will move also all the steps, but at different speeds. So, smoothing occurs also or a smooth surface can be preserved. This has importance when thinning of interfaces is made.

Inhomogeneous samples

As a conclusion, during ion milling of a homogeneous material, the sample must be rotated to produce a smooth, polished surface. However, if the sample is not homogeneous, e.g. a polycrystal, a composite or a cross section of a film on a substrate is being thinned, then no smooth surface can be created because in differences in $V(\theta)$. Rather a faceted surface, composed from smooth plateaus, separated by steps above the interfaces will form. In this case a wedge of the angle α develops at the interface (fig. 6.), which makes the electron microscopic investigation of the interface and/or the film difficult, because the interface will be superimposed on a wedge, step-like or less abrupt, of the thinned area. The slower sputtering material can even be too thick for transmission investigation in TEM. The wedge angle α depends on $SR(\alpha, \theta)$ of the material having lower sputtering rate, and on the sputtering rates of the two components:

$$\operatorname{tg} \alpha = \frac{V_2(\theta) - V_1(\theta)}{V_1(\theta) * SR_1(\alpha, \theta)} \quad (4)$$

For example, if $V_1(\theta)=40$ mm/h and $V_2(\theta)=10$ mm/h and $SR(\alpha, \theta)=10$, then the wedge angle of the sample will be close to 45° , 22° on each side.

To decrease the wedge angle $SR_1(\alpha, \theta)$ must be increased (fig. 5c.). $SR_1(\alpha, \theta)$ can be increased by changing the movement of the sample relative to the ion beam., i.e. the sample, instead of being

rotated, must be rocked or remain stationary, positioning the interface perpendicular to the grazing incidence ion beam. As a result, α of the facet at the interface will be decreasing. Another consequence is, that the facets on the surface of both positive and negative inclination angles, among those that one, which is located at the investigated interface, will be moving in the direction of the ion beam, since $SR(\alpha,\theta)$ is positive for both positive and negative α (fig. 5c). Due to this behavior, surface topography is both smoothed on one hand, and translated as a hole in the direction of the beam on the other. As it follows from fig. 5c., the steps having facets of small angle of inclination, located at the interface will move at a sufficiently high lateral speed in the ion beam direction, being pushed away from the interface. Instead, the morphology of the smooth area, adjacent to the interface on the surface will be translated over the interface, resulting in a smooth region at the location of the interface in the sample and a smaller α , corresponding to the larger value of $SR(\alpha,\theta)$. However, due to the very low angles of incidence the thickness of the sample hardly changes. This means, that the rocking or stationary sample can only undergo a surface morphology change but not efficient thinning. So thinning has to be carried out previously, in the beginning of the ion milling procedure, and the sample is usually rotated during this time. Then, in the very end of the milling process, when the sample is sufficiently thin and the surfaces are smooth in the homogeneous areas, rocking or stationary thinning can be used.

For a stationary sample also a fiber like artificial morphology develops on the sample surface. The fiber like structure is created because the inclined steps are moving only in the direction of the ion beam and not in the perpendicular direction. These artifacts can be eliminated by applying the rocking technique. In this case the sample is oscillated around the surface normal at $\pm\omega$ measured from the direction of the beam.

Similar effects can be achieved by shielding the samples from thinning in the direction of the interface [12] as well as by modifying the sample rotation speed so, that thinning in the direction of the interface is short compared to the thinning time in the perpendicular direction [13].

These theoretical considerations are reviewed in fig. 7, where different relative positions of the sample and of the ion beam direction are sketched [1].

PRACTICAL SAMPLE PREPARATION

The samples must be embedded, mechanically thinned and polished to about 50 μm thickness. A Ti disc, having a window (1.5x2 mm^2 e.g.) can be used for embedding, providing easy fixing of the crystals in the disc and good heat conduction (fig. 8.). The light emission of Ti under ion beam facilitates the positioning of the focused ion beam to the center of rotation of the sample. The

relatively slow sputtering speed of Ti provides a fairly strong rim to protect and aids handling the sample.

No dimpling is preferred for really low angle milling, since it will limit the lowest angle of incidence. For embedding of hard coatings on polycrystalline or other inhomogeneous substrates a piece of homogeneous material e.g. single crystalline Si should be used as a material, facing the film. Important moment is the conservation of parallelness of the mechanically polished surfaces. For this purpose special micrometer driven tools are preferred, which provide a possibility to mechanically thin the samples below 10 μm [14] substantially shortening the time required for ion milling.

The general ion milling procedure is the following. The mechanically polished sample is ion milled from one side by applying two ion guns in mirror position, operated at 10 kV with Ar^+ ions. The ion beam incidence angle is lower than 5° and the sample is rotated. This step is used to remove the half of the thickness and create a smooth, ion-polished surface. After this step, the ion beam incidence angle is lowered below 5° and the sample is oscillated around its surface normal at $\pm\omega$ measured from the direction of the beam, aligned perpendicularly to the interface in question. By applying one ion gun operated at 10 kV the wedge shape surface at the interface is pushed away from the interface area, and onto the new surface with lower angle of inclination a smooth surface morphology is moved in from the adjacent terrace area. This process is continued until the steeper wedge is moved far enough from the interface to be investigated. This must be decided by inspection through the optical microscope of the thinning unit. After finishing the sputtering on one side, the same procedure is repeated to the other. On the second side ion milling with rocking is continued until the perforation of the sample takes place and the hole is brought close to the interface.

Two main strategies can be applied in using the rocking method:

The first when one applies the ion beam from the opposite direction for sputtering the first and second side of the sample. With this technique, the thickness of the sample at the interface will be homogeneous (fig. 7b.). However, perforation might take place on both sides of the interface creating a bridge and in this way making the heat conduction poor at the interface area. Another disadvantage of this technique is, that the edge of the perforation in front of the interface is hit by the beam, resulting in sputtering away quickly the thinnest parts.

The second technique is, when one applies the ion beam from the same direction for both sides of the sample. Although in this case the thickness of the sample will not be homogeneous, the perforation is created behind the harder component resulting in a very sharp wedge (fig. 7a.).

The type of strategy to be applied should be decided by the user according to the characteristics of the sample and glue, used to embed the sample..

Creation of artifacts during ion beam thinning.

During ion beam thinning an amorphous layer develops on the sample surface and the thickness of this layer is in the range of the penetration depth of the incident ions. Therefore the thickness of this altered layer can be reduced by lowering the ion beam incidence angle and the ion energy. Using Auger depth profiling measurements of nm multilayers it could be shown that the interface sharpness and signal amplitude increases dramatically if the ion energies are lowered [15]. The measurements have been done for 1 and 0.4 keV sputtering Ar⁺ ions. At usual procedures the ion energy is lowered to 3 keV (from 10 keV for a few minutes in the end of the thinning).

Beyond the creation of the altered layer other artifacts are also produced during ion beam sputtering like dislocation loops and point defect clusters. The appearance of these artifacts can hinder the detailed investigation of the microstructure. The density of these artifacts could be reduced by applying low energy ion beam sputtering at the end of the thinning process. This has been tested in the case of W. Comparing the results after sputtering with 3 keV and 0.5 keV ion energy at 84° ion beam incidence angle, one finds that the defect density is reduced considerably, however, the artifacts do not disappear even at 0.5 keV ion energy.

To illustrate the power of this method the cross section image of a 10 μm thick diamond film on Si is shown. The sample was prepared by using extremely low angle ion milling (Ar⁺, 10 kV), utilizing also the retarding field arrangement for decreasing the angle of incidence. Both the film and the substrate are thin and transparent for 200 keV electrons, showing no disturbing thickness effects (fig. 9.). The diamond/Si interface as well as the grain and surface structure of the film can be investigated at high resolution. Actually the film structure shows growth competition among the grains, the slower growing grains are lost from the structure as the film thickness increases. There is an undefined sublayer at the substrate surface of about 200 nm thickness. The growth starts with a small grain size, of about 1 μm, which reaches a grain width of about 2-5 μm at the surface of the film. The surface grains are faceted, resulting in a relatively rough surface. Facets as large as 1-2 μm are present.

SUMMARY

Embedding a harder and a softer material, the softer can be the substrate or an added backing (single) crystal. makes possible that during low angle ion milling in combination with sample rocking and surface morphology translation smooth and thin areas of these structures can be prepared for TEM investigation. The knowledge from the geometric theory of surface morphology development

during ion milling together with sample preparation techniques as well as the appropriate ion milling arrangement is an efficient technology of preparing good samples of composites of hard and soft materials, the hard material being in the form of a thin or thick film on a substrate, fibers or powders.

ACKNOWLEDGMENT: The projects of the National Science Foundation (OTKA014091 and OTKAT15378) are acknowledged for financial support.

REFERENCES

1. Á. Barna: Mat. Res. Soc. Symp. Proc. Ser. 254 (1992) 3.
2. G. Radnóczy and Á. Barna, Proc. of E-MRS 1995 Spring Meeting to be published in Surf. and Coatings Techn. 1996.
3. J. P. McCaffery, Microscopy Research and Technique 24, 1993, 180.
4. A. Ourmazd, Materials Science Reports, 9 (1993), 201.
5. R. Cong-Xin, C. Guo-Ming, F. Xin-Ding, Y. Jie, F. Hong-Li and T. Shih-Chang: Radiation Effects, 77 (1983) 177.
6. C.W. Bulle-Lieuwma and P.C. Zalm: Surf. and Interface Analysis, 10, (1987), 210.
7. G.K. Wehner: J. Vac. Sci. Technol. A3 1 (1985) 821.
8. J.A. Kubby and B.M. Siegel: Nuc. Instr. and Met. in Phys. Res. B13 (1986) 319.
9. H.J. Roosendaal: in Sputtering by Particle Bombardment I, Ed.: R. Behrisch, Springer-Verlag Berlin (1981).
10. M.A. Tagg, R. Smith and J.M. Walls: Journal of Mat. Sci. 21 (1986) 123.
11. H.H. Andersen and H.L. Bay: in Sputtering by Particle Bombardment I, Ed.: R. Behrisch, Springer-Verlag Berlin 1981.
12. U. Helmersson and J.-E. Sundgren: Journal of Electron Microscopy Technique, 4 (1986) 361.
13. F. Shaapur and K.A. Watson: Mat. Res. Soc. Symp. Proc., 254 (1992) 153.
14. S. J. Klepeis, J. P. Benedict, R. M. Anderson, in Specimen Preparation for Transmission Electron Microscopy of Materials, MRS Proc. 115, ed. by Bravman, p.179.
15. Á. Barna, M. Menyhárd, Phys.Stat. Sol. (A) 145 (1994) 263

FIGURE CAPTIONS

- Fig. 1. The basic surface elements of the model are inclined macro facets, separating the smooth surface plateaus creating surface steps.
- Fig. 2. Arrangement of ion milling geometry. The coordinate system XYZ is fixed to the ion guns, xyz is fixed to the sample.
- Fig. 3. The dependence of the relative sputtering speed $V(\theta)/V(0)$ on the ion beam incidence angle.
- Fig. 4. Schematic drawing of the ideal shape of the $SR(\alpha, \theta)$ curve for rotating (a) and rocking (b) sample movement.
- Fig. 5. Calculated $SR(\alpha, \theta)$ curves for Si. a) general behavior at different angles of incidence, b) behavior in the grazing angle of incidence range, c) effect of sample movement on $SR(\alpha, \theta)$.
- Fig. 6. Development of wedges at the interface of materials having different $V(\theta)$. a) $V_1(\theta) < V_2(\theta)$, b) $V_1(\theta) > V_2(\theta)$.
- Fig. 7. Development of the sample cross-section during rocking. a) $V_A(\theta) = V_C(\theta) > V_B(\theta)$, the sample perforates in A at one or both points marked K. The development of a bridge structure is probable b) $V_A(\theta) = V_C(\theta) > V_B(\theta)$, perforates in A behind the A/B interface at the point marked K.
- Fig. 8. The geometry of embedding sample materials into the Ti disc for mechanical preparation.
- Fig. 9. Electron micrograph of 10 μm diamond film on Si.

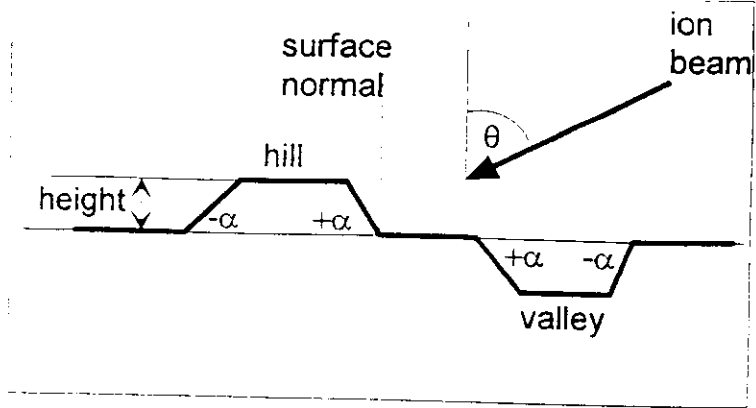


Fig. 1.

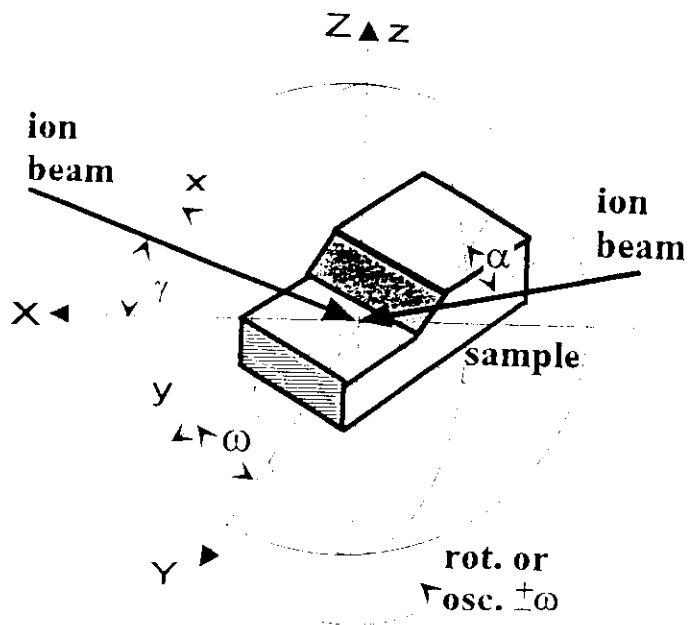


Fig. 2.

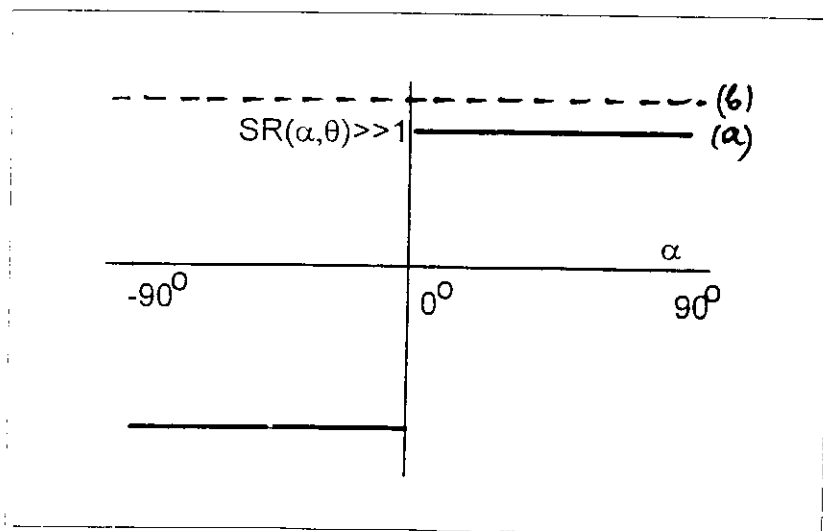


Fig. 4

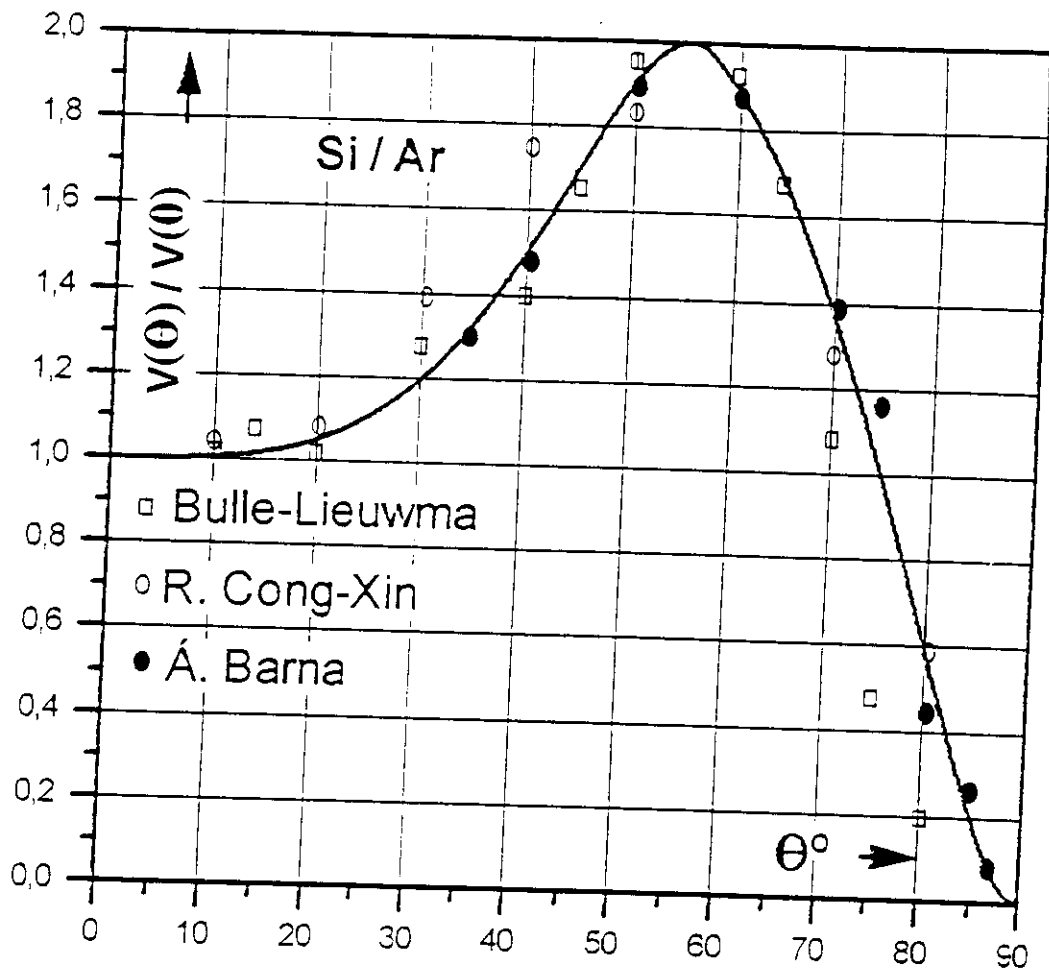
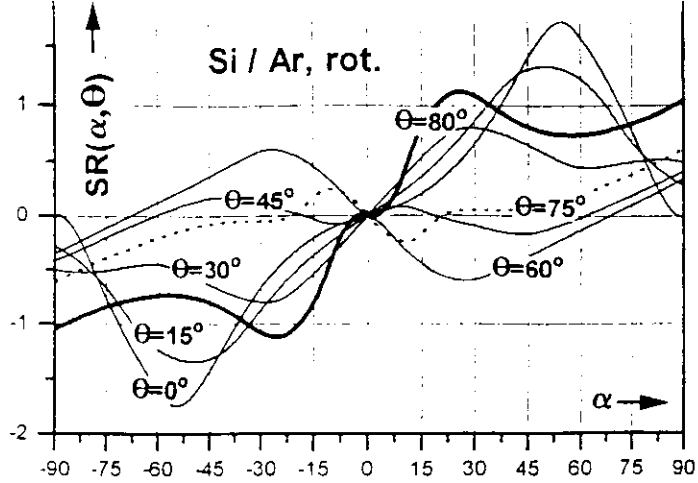
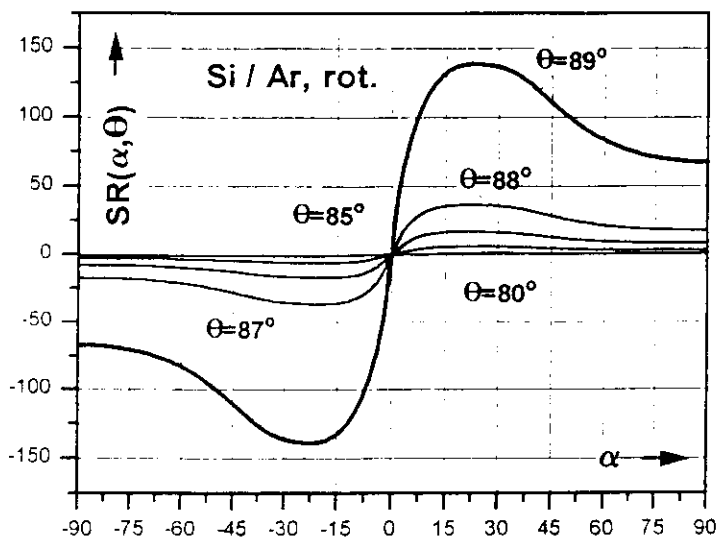


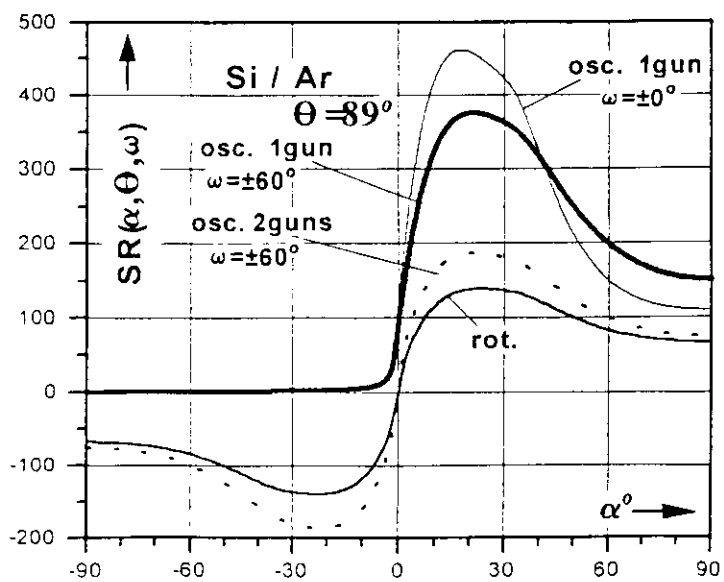
Fig. 3.



a



b



c

Fig. 5.

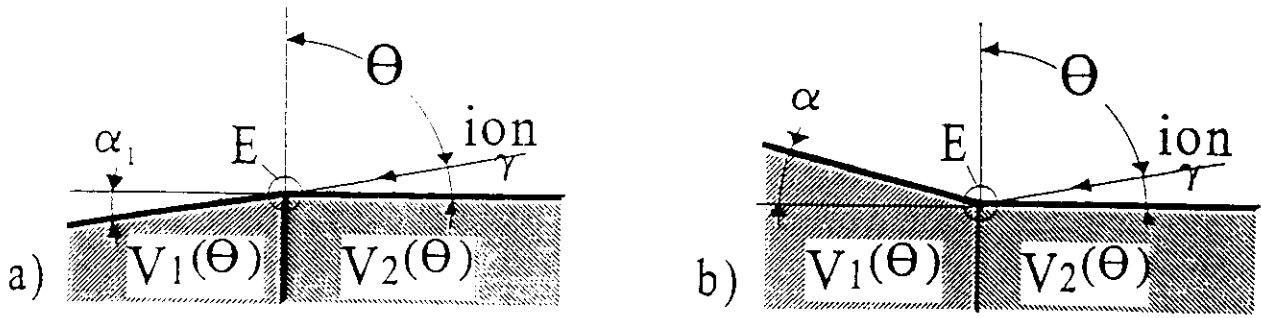


Fig. 5

Fig. 6.

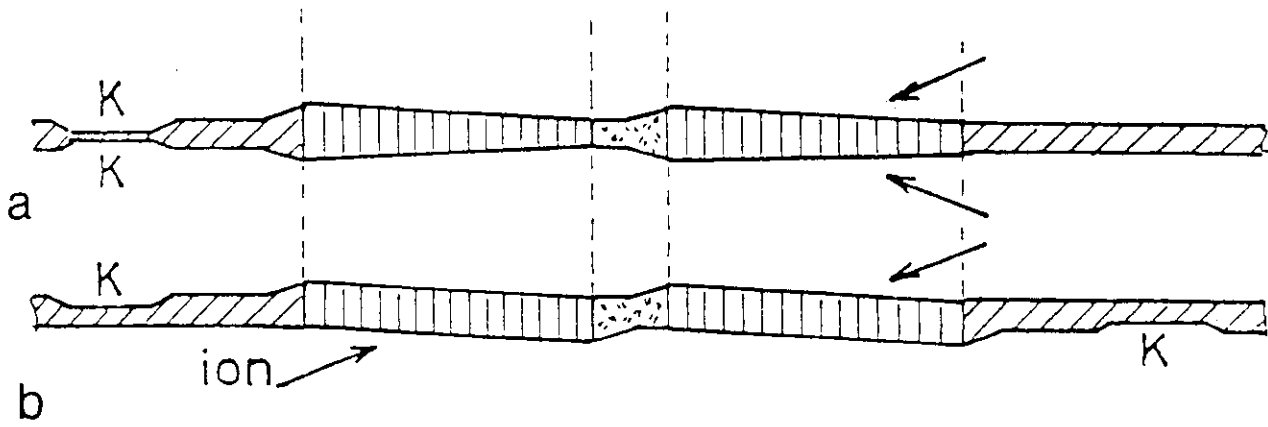


Fig. 7.

Fig. 6

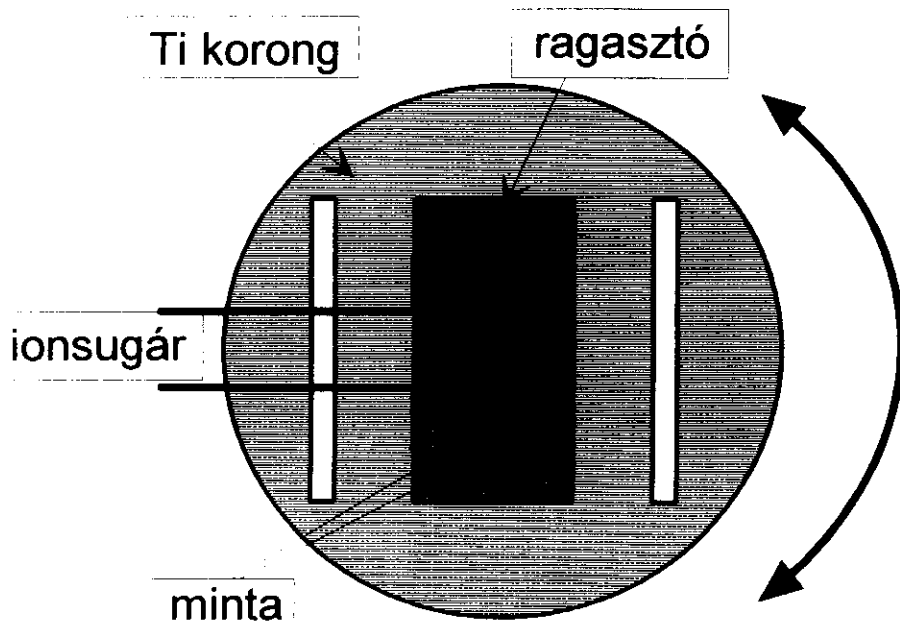


Fig. 8.



Fig. 9

A Novel Method for the Cross-Sectional TEM Preparation of Thin Films Deposited Onto Water-Soluble Substrates

GYÖRGY SÁFRÁN AND PIERRE PANINE

Research Institute for Technical Physics of the Hungarian Academy of Sciences, Budapest H-1325, Hungary (G.S.); Université Joseph Fourier Secretariat D.E.A. Maison des Magistères, 38042 Grenoble Cedex, France (P.P.)

KEY WORDS Water-soluble substrate, Replacement of film, Ion beam thinning

ABSTRACT A preparational method was developed solving the problem of cross-sectional TEM preparation of thin films and layer systems deposited onto water-soluble substrates. The technique is based on the replacement of the sample onto steady substrate, followed by mechanical and ion beam thinning. Cross-sectional TEM micrographs of Ag and Ag/Ag₂Se layers are shown presenting the efficiency of this novel technique. © 1993 Wiley-Liss, Inc.

INTRODUCTION

NaCl single crystal substrates are widely used for lateral TEM investigation of vacuum deposited layers and layer systems, allowing simple preparation by wet-stripping and placing the deposits onto microgrids prior to TEM investigation. Cross-sectional transmission electron microscope (XTEM) investigation of layers deposited onto NaCl substrates, however, has a great difficulty. A publication by Heuer and Howitt (1990) reported on the XTEM preparation of TiO₂ films evaporated onto NaCl by using microtomy. The disadvantage of this method is the high concentration of crystal defects generated by the mechanical treatment; moreover, the films often break into small parts.

Our aim was the XTEM investigation of solid phase reaction between single crystalline Ag films and selenium subsequently deposited onto NaCl. As the conventional ion beam XTEM preparation (Abrahams and Buocicchi, 1974) includes wet grinding and polishing, the high water-solubility of NaCl turns to be disadvantageous. The essential demand that the substrate remain solid during and after cross-sectional preparation and support the sample to be investigated is not fulfilled in case of NaCl. For solving this problem we developed a method for XTEM preparation of thin layers and layer systems detached from their substrates.

MATERIALS AND METHODS

Our method is convenient for cross-sectional preparation of thin films which can be detached from their substrates, can be treated with the conventional mechanical polishing methods, and are resistive to a heat treatment applied to the polymerization of the embedding agent. The stages of preparation are shown in Figure 1.

The NaCl substrate together with the thin deposited layer was first cleaved into parts having lateral sizes about 2 × 2 mm. Pieces of the layer were wet-stripped, picked up by a platinum wire loop (Fig. 1a), and placed onto two small silicon slabs having dimensions about 1.8 × 0.8 × 0.3 mm. The slabs were previously fixed onto filter paper by pieces of adhesive carbon film. As the two slabs together with the thin layers on their top surfaces became dry, they were put face to face into the

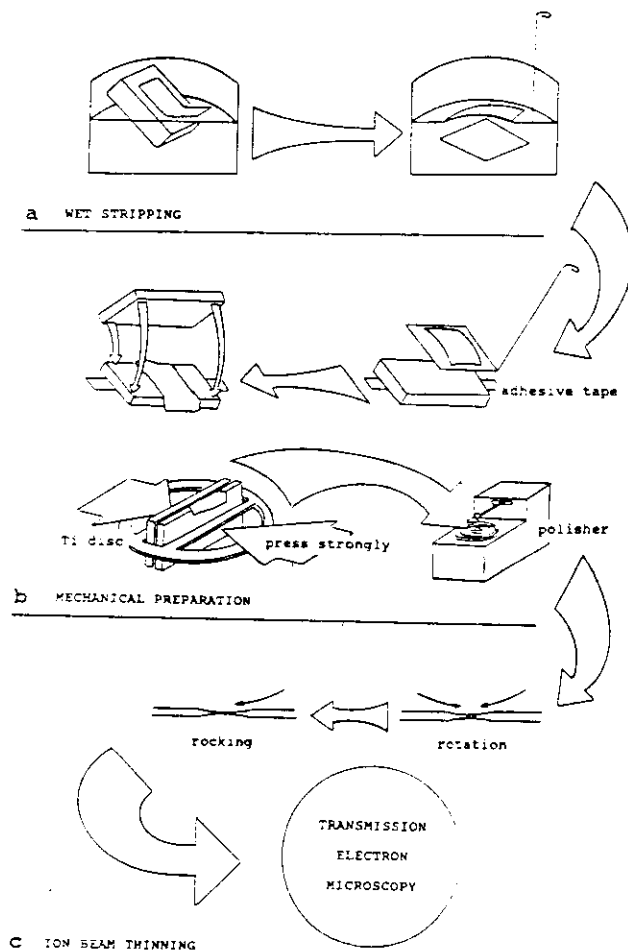


Fig. 1. Schematic diagram of the stages of cross-sectional preparation of thin samples detached from their substrates. a: Wet stripping. b: Embedding and mechanical thinning. c: Ion beam thinning.

Received October 29, 1992; accepted in revised form February 12, 1993.
Address reprint requests to György Safran, Research Institute for Technical Physics, Hung. Acad. Sci., H-1325 Budapest, P.O.B. 76, Hungary

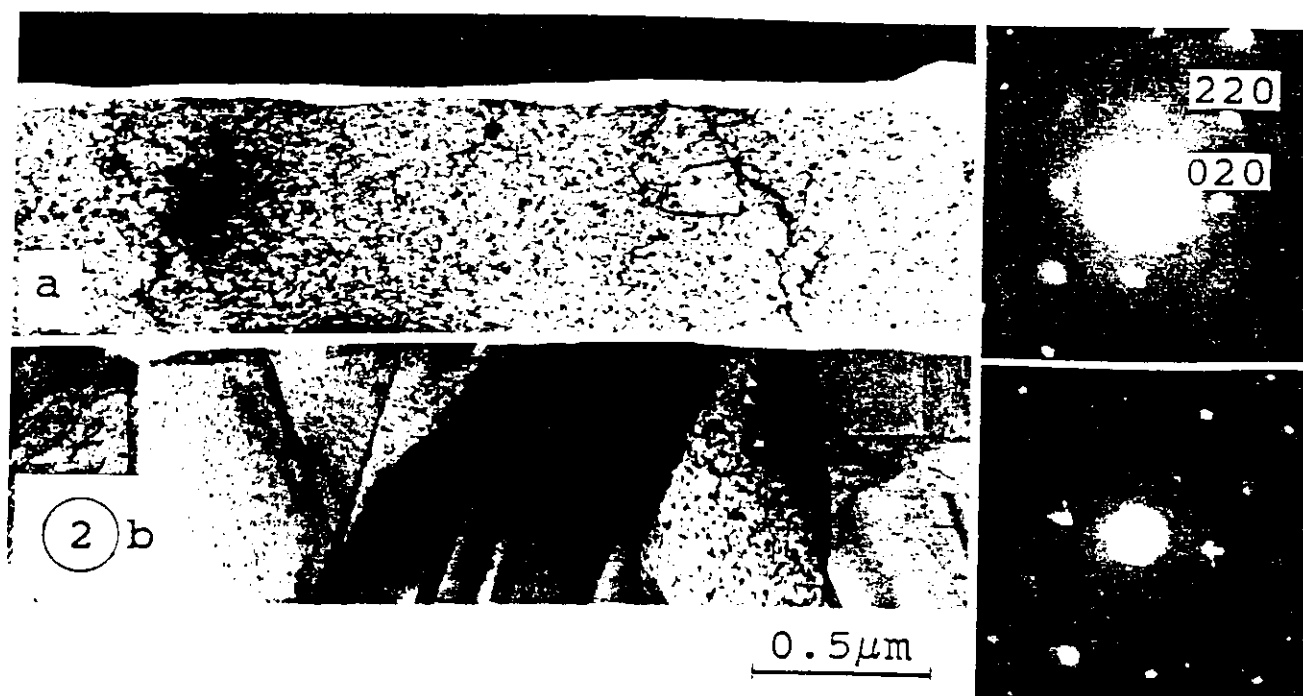


Fig. 2. Cross-sectional TEM view of (a) (100) oriented monocrystalline Ag film and (b) polycrystalline Ag film simultaneously deposited onto pretreated NaCl and Si substrates, respectively. Insets: Corresponding SAED patterns. As a calibration reflexes of Ag 020 and 220 are indexed in a.

slot of a specially shaped Ti disc (Barna, 1991). They were pressed together and cemented into the disc by a mixture of Araldite 600 and carbon powder (Fig. 1b). The resin was polymerized by heat treatment at 160°C for 2 h.

The cross-sectional mechanical thinning of the samples was carried out using a Micropol MC56 polisher produced by the Research Institute for Technical Physics of the Hungarian Academy of Sciences. First grinding with 600 grit SiC abrasive paper was applied, followed by polishing with wet suspension of 1 μm size AlO₃ powder. The thickness of the sample was approximately 50 μm after the mechanical polishing.

The thinning was continued by ion milling using Teletwin ion guns (Barna, 1984). The samples were first rotated, and bombarded simultaneously by two guns operating at 10 kV. The incident angle of the ion beams was about 3–5° to the sample surface. Finally rocking movement of the sample in a 120° range and bombardment with single gun was applied (Fig. 1c). During the last 5 min the accelerating voltage of the Ar⁺ ions was reduced to 3 kV. This technique of ion milling reported earlier by Barna and Barna (1989) and Barna (1991), enabled the preparation of a large transparent area of the sample at the region of interest.

The thinned samples were investigated using a Philips CM20 transmission electron microscope operating at 200 kV.

RESULTS AND DISCUSSION

The efficiency of this preparational technique is represented in Figures 2 and 3. The cross-sectional view of a (100) oriented and a polycrystalline silver layer deposited simultaneously onto NaCl and Si substrate is shown in Figure 2a,b, respectively. The NaCl substrate of the film shown in Figure 2a was treated with bidistilled water and chlorine gas prior to deposition in order to get epitaxial orientation. This kind of pretreatment of NaCl cleavages was reported by Sáfrán et al. (1993). The substrate of the film shown in Figure 2b was a Si wafer covered with SiO₂. The two layers were embedded and thinned together so that the polycrystalline film deposited onto the Si substrate supported the single crystalline one which was previously wet-stripped from the NaCl. It is clearly shown that due to this preparation technique the layers are situating very close to each other and have contact at many points. However, no traces of the embedding araldite was found in between the two layers; the sample was stable enough. This is attributed to both the presence of embedding material on the other side of the single crystalline film (upper side of Fig. 2a) and the adhesion to the supporting substrate. It is noteworthy that direct comparison of the two simultaneously deposited and thinned layers pointed out that the thickness of the single crystalline film was 671 nm, while that of the

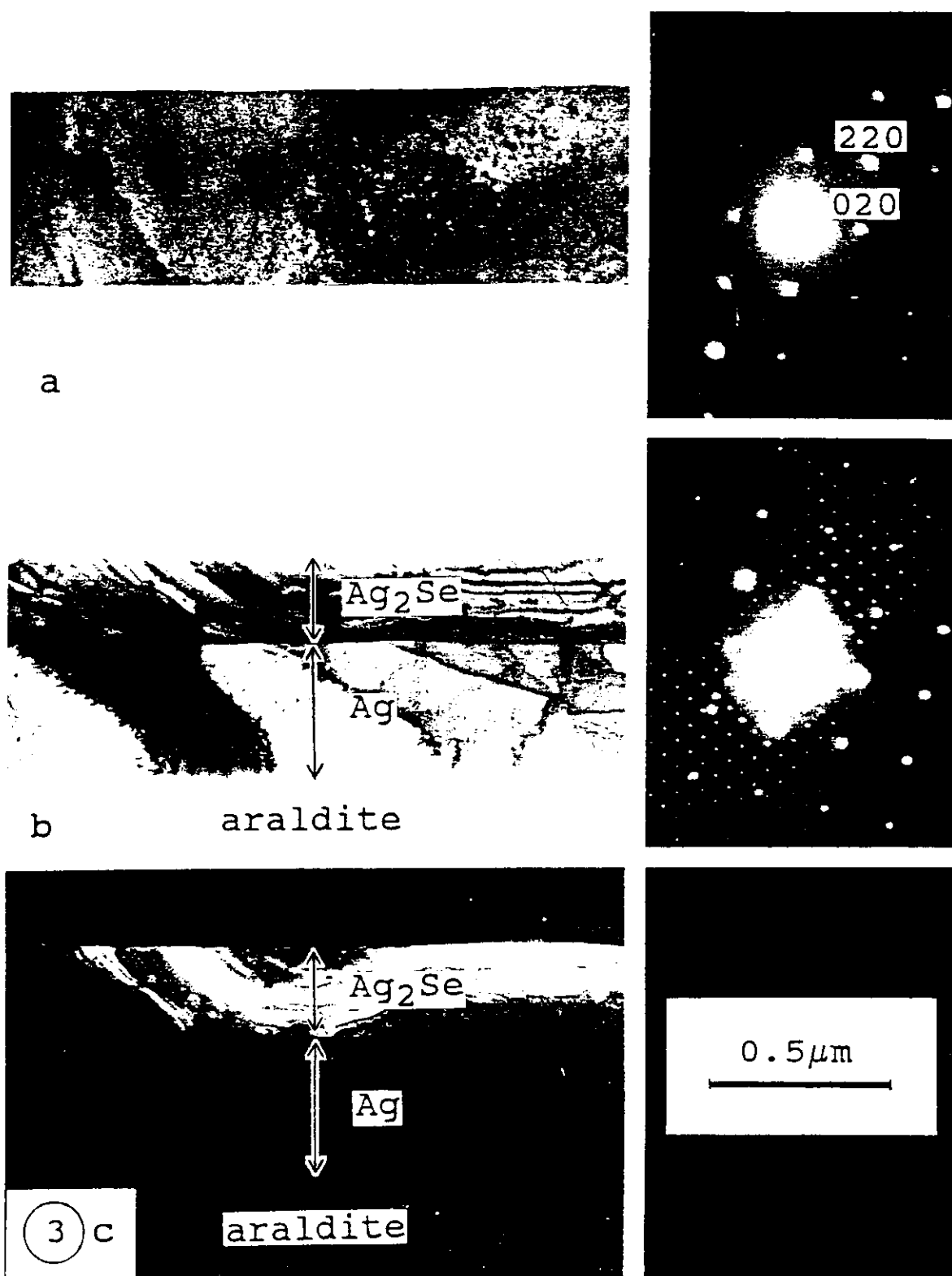


Fig. 3. Cross-sectional TEM view of (a) (100) oriented single crystalline silver layer deposited onto pretreated NaCl, (b) the same as a reacted with 200 nm of selenium, and (c) dark field micrograph taken

with an Ag_2Se reflexion from the same area shown in b. Insets: Corresponding SAED patterns. As a calibration reflexes of Ag 020 and 220 are indexed in a.

polycrystalline one was 746 nm. The thickness difference of 11% is supposed to arise from the different sticking coefficients of Ag adatoms arriving onto both the two different substrates and onto the Ag surfaces having different orientation and morphology. A lower density of the polycrystalline film is considered another explanation (Nagatani and Saito, 1989).

Figure 3 represents another specimen investigated by using this preparational method. In this sample the solid phase reaction between a single crystalline Ag layer deposited onto NaCl substrate and selenium vapour was investigated in cross-section. Figure 3a-c shows an unreacted silver layer having a thickness about 500 nm, a silver layer reacted with 200 nm of selenium, and a dark field (DF) image of the same area, respectively. Both thicknesses have been measured with a quartz thickness monitor during vacuum deposition. The DF image was taken by using one of the diffracted beams arising from the Ag_2Se phase. Both bright and dark field images represent a flat and smooth interface between reacted and unreacted areas (Fig. 3b,c). Different patterns of bending contours can be seen in the silver and silver-selenide sublayers. Measurements carried out on the negatives of cross-sectional micrographs shown in Figure 3 enabled the determination of the geometry of both Ag and partly selenized Ag films: the original thickness of the Ag layer was found to be 552 nm (Fig. 3a). After reacting it with the selenium, the entire thickness of the layer (which is now a bylayer) increased to a value of 669 nm. The interface between reacted and unreacted regions is situated at a depth of 268 nm, leaving 401 nm of silver intact (Fig. 3b,c). Consequently 151 nm of silver participated the reaction.

Considering the crystallographic data that the reaction product (Ag_2Se) has a volume 1.74 times higher than the involved parent crystal (silver), the thickness of the silver-selenide layer should be $151 \text{ nm} \times 1.74 = 262 \text{ nm}$. This is in a good agreement with the value (268 nm) measured on the negatives.

Detailed cross-sectional investigations on the mech-

anisms of the Ag-Se reaction in single- and polycrystalline silver films will be published elsewhere (Panine and Sáfrán, 1993).

CONCLUSIONS

The simple preparational method represented in this paper proved to be very effective in the cross-sectional TEM studies of thin films detached from their substrates. It is very convenient for investigations carried out on thin single crystalline layers deposited onto NaCl. This preparation technique makes possible the investigation of thin layers and layer systems developed due to solid phase reactions. As more samples can be embedded and thinned simultaneously, it enables the direct comparison of geometrical, morphological, structural, and compositional properties of different samples in one cross-sectional view.

REFERENCES

- Abrahams, M.S., and Buoicchi, C.J. (1974) Cross sectional specimens for transmission electron microscopy. *J. Appl. Physiol.*, 45:3315-3316.
- Barna, A. (1984) A new type of ion milling equipment for sample preparation. In: *Proceedings of the 8th European Congress of Electron Microscopy*, Budapest, Vol. 1. A Csanády, P. Röchli, and D. Szabó, eds. Pp. 107-108.
- Barna, A. (1991) Topographic kinetics and practice of low angle ion beam thinning. In: *Mat. Res. Soc. Symp. Proc.*, Vol. 254. R. Anderson, B. Tracy, and J. Bravman, eds. Mat. Res. Soc., Pittsburgh, Pennsylvania. Pp. 3-22.
- Barna, A., and Barna, P.B. (1989) Model considerations of ion beam thinning for preparing TEM samples. In: *Proceedings of the 3rd Balkan Congress on Electron Microscopy*, Athens. Lukas H. Margaritis, ed. Pp. 246-249.
- Heuer, J.P., and Howitt, D.G. (1990) A novel technique for the preparation of thin films for cross-sectional transmission electron microscopy. *J. Electron Microsc. Tech.*, 14:79-82.
- Nagatani, T., and Saito, S. (1989) Development of a high resolution SEM and comparative TEM SEM observation of fine metal particles and thin films. In: *Proceedings of EMAG-MICRO 89*. London, Institute of Physics, Bristol, New York. Pp. 519-522.
- Panine, P., and Sáfrán, G. (1993) In situ electrical and cross sectional TEM studies on the selenization of silver films. *Thin Solid Films* (in press).
- Sáfrán, G., Barna, P.B., Geszti, O., and Günter, J.R. (1993) The role of chlorine adsorption in the low temperature epitaxial growth of Ag, Au and Cu on air cleaved NaCl. *Thin Solid Films* (in press).